SUPPORTING INFORMATION

Fragmentation patterns of DNA-stabilized silver nanoclusters under mass spectrometry

Rweetuparna Guha[a], Sami Malola[e], Malak Rafik[a], Maya Khatun[e], Anna Gonzàlez Rosell[a], Hannu Häkkinen[e], Stacy Marla Copp[a,b,c,d]

[a] *Department of Materials Science and Engineering, University of California, Irvine, CA 92697, USA*

[b] *Department of Physics and Astronomy, University of California, Irvine, CA 92697, USA*

[c] *Department of Chemical and Biomolecular Engineering, University of California, Irvine, CA 92697, USA*

[d] *Department of Chemistry, University of California, Irvine, CA 92697, USA*

[e] *Departments of Chemistry and Physics, Nanoscience Center, University of Jyväskylä, Jyväskylä 40014, Finland*

*Correspondence to stacy.copp@uci.edu

Table of Contents

1 General methods and materials.

***Materials*.** DNA oligomers were purchased from Integrated DNA Technologies (standard desalting). Silver nitrate (99.9999%, Sigma Aldrich) and ammonium acetate (99.8% Fisher Scientific) were used. All the samples were prepared in MilliQ ultrapure water.

2 Synthesis and purification of Ag_N-DNAs.

A stoichiometric amount of $AgNO_3$ was added to the ssDNA oligomer in 10 mM ammonium acetate (pH 7) to form the Ag^+–DNA complex. After 15 minutes, a freshly prepared aqueous solution of $NaBH_4$ ($[BH_4^-]/[Ag^+] = 0.5$) was added to the Ag^+–DNA complex. Samples were stored at 4 °C in the dark for 3-5 days, allowing sufficient time for the Ag_N-DNA formation. The stoichiometry for Ag^+:DNA was optimized for each Ag_N-DNA to achieve maximum chemical yield. No additional chloride source was added to synthesize chlorido-protected ***Group III*** Ag_N-DNAs. The Ag_N-DNAs were purified using ion-paired reverse-phase high-performance liquid chromatography (HPLC) on Agilent 1260 Infinity. The original fluorescence detector (FLD) was replaced with a Hamamatsu R13456 photomultiplier tube (PMT) to achieve higher sensitivity > 600 nm, providing 250 times signal enhancement at 750 nm. We used a Kinetex C18 column with 100 Å pore diameter, 5 μm particle size, and 50 mm × 46 μm dimensions (Phenomenex). The solvents used were MilliQ H_2O and MeOH containing 35 mM triethyl ammonium acetate (TEAA, pH = 7.0) as an ion-pairing agent. The *in-situ* absorbance spectra recorded by the diode-array detector (DAD) and the fluorescence spectra (FLD) confirm the collection of the fluorescent product of interest. After purification, samples were solvent exchanged into 10 mM ammonium acetate using 3 kDa spin filters (Amicon, Millipore Sigma). The synthesis and purification conditions and HPLC chromatograms of Ag_N-DNAs are previously reported.[1-4]

Table S1. Synthesis conditions and purification of **I.8**.

Name	DNA Sequence (5'-3')	[DNA]	[$AgNO_3$]	Abs / nm	Em / nm	HPLC gradient % of 35 mM TEAA in MeOH, 10 min	Time of elution / min
***I*.8**	GTAGTCCCTA	20 μM	100 μM	554	732	12-27%, 1 mL/min	2.78 - 2.86

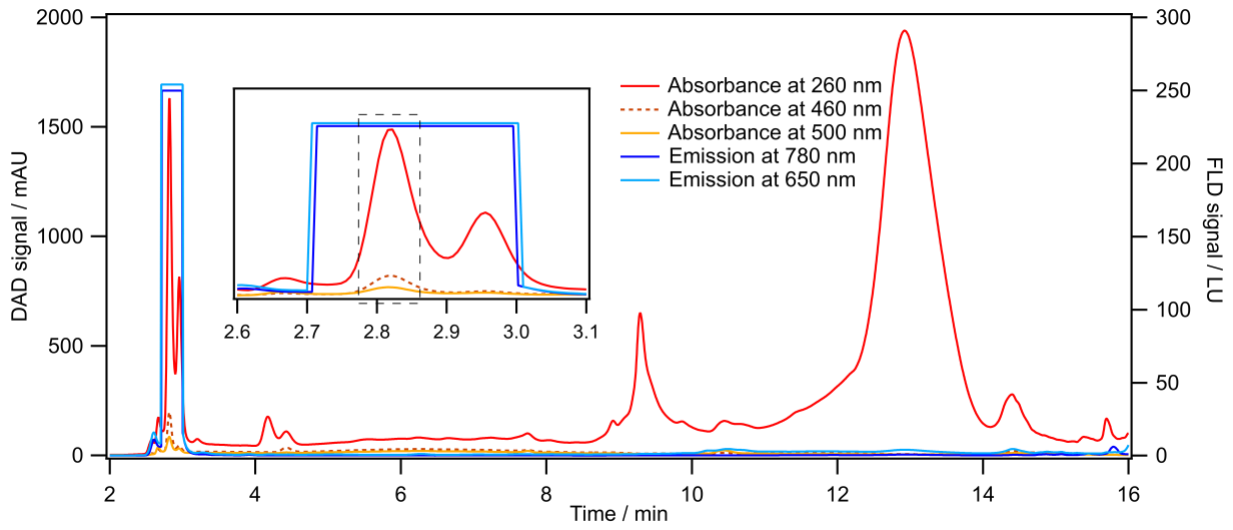

Figure S1. HPLC chromatogram of ***I*.8**. The dashed line shows the collected fraction. DAD signals correspond to absorbance through the DNA nucleobases (260 nm, red), and absorbance through the nanocluster of interest (500 nm, orange). FLD signals correspond to the emission wavelengths of the product of interest (780 nm).

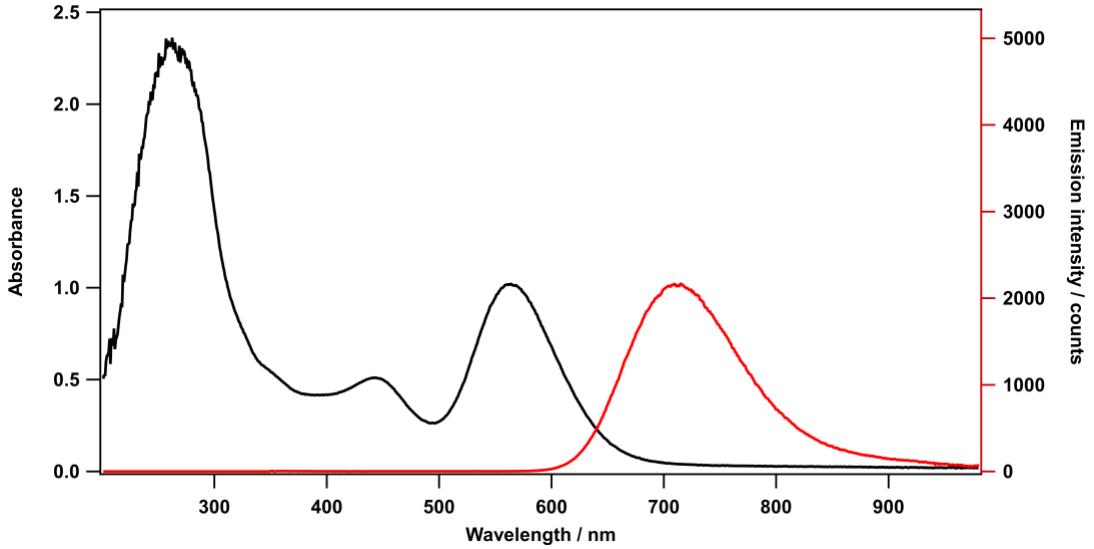

Figure S2. Absorbance and emission spectra of HPLC purified ***I*.8**.

3 Mass spectrometry.

HPLC-purified Ag_N-DNAs were solvent exchanged to 10 mM ammonium acetate (pH 7) and were directly injected at 100 µL/min in negative ion mode with a 2 kV capillary voltage, 30 V cone voltage, and no collision energy. Spectra were collected from 1000 to 4000 *m/z* and integrated for 1 s. Unless otherwise stated, the source and desolvation temperatures were 80 and 150 ºC

(otherwise noted, see **Fig. S22**), respectively. Gas flows were 45 L/h for the cone and 450 L/h for the desolvation. Samples were injected with 50 mM NH_4OAc – MeOH (80:20) solution at pH 7.

3.1 Determination of the molecular formula of Ag_N-DNAs.

Determination of N_{Ag}, N_0, and n_s:

High-resolution ESI-MS allows the determination of the ion mass to charge ratio, *m/z*, as well as *m* and *z* by resolving the isotopic distribution of the product. For compositionally pure Ag_N-DNAs, the experimentally measured ESI-MS isotope pattern is compared to the calculated distribution of the cluster and the numbers of silver atoms *N,* and the number of DNA strands n_s are determined. to separate *N* into effective neutral (N_0) and cationic (N_+) silver content *i.e.,*

$$N = N_0 + N_+$$

The charge state *z*– of a *m/z* peak is determined by the spacing between adjacent peaks of the isotope pattern, which are spaced by 1/*z*. The total charge of the complex corresponding to this *m/z* peak is equal to the charge of the number of silver cations, eN_+, minus the charge of the number of protons removed from the DNA, en_{pr}, to reach the total charge of $-eZ$ observed experimentally:

$$-ez = eN_+ - en_{pr} \quad (1)$$

Then, because *n*pr protons have been removed from the Ag_N-DNA complex, the measured total mass *m* (in amu) is:

$$m = m_{DNA}\, n_s + mAg\, (N_+ + N_0) - n_{pr} \quad (2)$$

where m_{DNA} is the DNA template strand mass, n_s is the number of DNA strands in the complex, and m_{Ag} is the silver atom mass (the mass of a proton is treated here as 1 amu). N_+ and N_0 may be determined by calculating the isotope distribution pattern for varying values of N_+, and thus n_{pr}, to determine the cluster charge (Q_c) that best matches the isotope pattern. The molecular formula of Ag_N-DNA is denoted as $(DNA)_{ns}(Ag_NCl_x)^{Qc}$. In the absence of Cl^- ligands, N_+ equals Q_c, whereas, in the presence of Cl^- ligands, $Q_c = N_+ - x$.

The nanocluster size and charge were determined by fitting the calculated isotopic distribution of the Ag_N-DNA to the experimental spectra. Calculated isotopic distributions were obtained from MassLynx using the chemical formula and corrected for the nanocluster's overall positive charge (oxidation state) cluster. The Ag_N-DNA composition and charge were determined by fitting the calculated isotopic distribution of the Ag_N-DNA to the experimental spectra. To

confirm the overall charge of the nanocluster (Q_c), we compared the best fit with the two observed charge states peaks, z = 4− (dark blue curve) and z = 5− (light blue curve) as shown in the insets of **Fig. S3** to **S20**.

Determination of the overall charge of the nanocluster (Q_c) to deduce the N_0.

To determine the overall charge of the nanocluster (Q_c), single Gaussians were fitted to the peaks that appeared in experimental mass spectra, and the centers (x_0) of these Gaussian fits were compared. The centers the Gaussian fits of the isotopic distributions calculated for a range of Q_c values generally include $Q_c = 0$, best fitted Q_c, and ± 1 values of centers fitted Q_c.

Once the Q_c is determined, N_0 is determined using the formula:

$$N_0 = N - Q_c \quad (3)$$

3.2 Mass spectra of Ag_N-DNAs.

The mass spectra and the detailed analysis of the molecular composition of Ag_N-DNAs **I.1** to **I.7**, **II.1** to **II.3**, and **IV.1**, **IV.4** can be found in Ref. 1 and 3, respectively.[1, 3] The detailed analysis of the mass spectra of **I.7** and **III.1** to **III.5** are reported in Ref. 2 and 4, respectively.[2, 4]

3.2.1 Mass spectra of *Group I* Ag_N-DNAs.

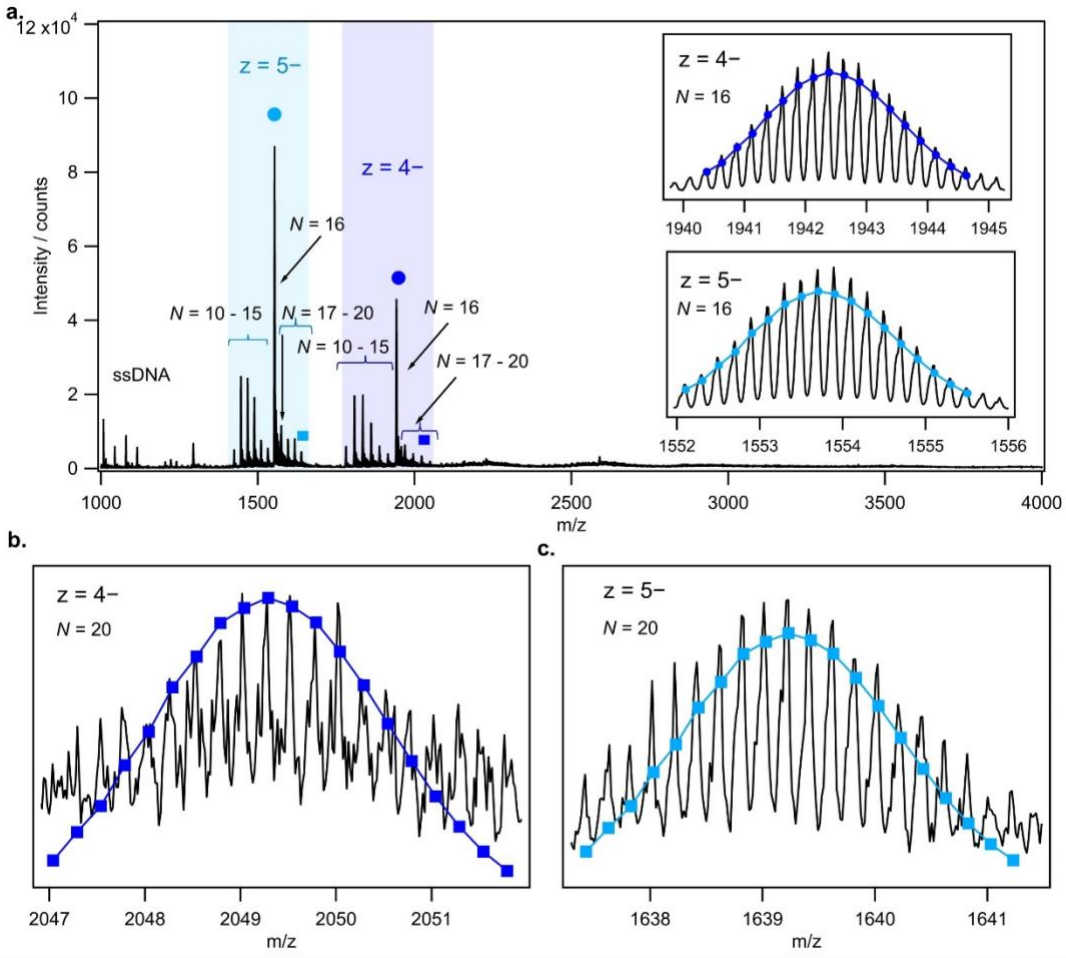

Figure S3. Mass spectra of ***I*.1**. **a**) Experimental isotopic distributions (black curves) for all peaks of ***I*.1** mass spectra. Insets show isotopic distributions aligned with experimental peaks for $(DNA)_2[Ag_{16}]^{10+}$ at z = 5− (light blue, circled) and z = 4− (deep blue, circled) for the peaks with the highest intensity. **b**) and **c**) Isotopic distributions with experimental peaks for $(DNA)_2[Ag_{20}]^{14+}$ at z = 4− (deep blue, squares) and z = 5− (light blue, squares), respectively. Isotopic distributions were calculated using the chemical formula $C_{192}H_{244}N_{78}O_{116}P_{18}Ag_{16}$ (**a**. insets) and $C_{192}H_{244}N_{78}O_{116}P_{18}Ag_{20}$ (for **b.** and **c.**), respectively. Reproduced from Ref. 1.[1]

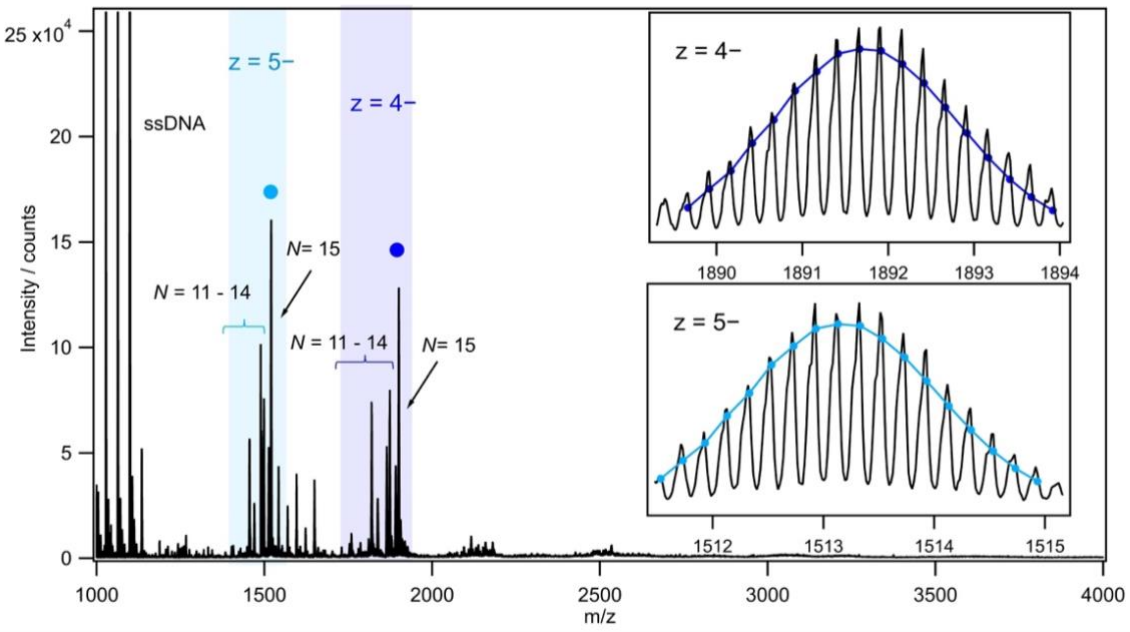

Figure S4. Mass spectra of ***I.2.***[4] Experimental isotopic distributions (black curves) for all peaks of ***I.2*** mass spectra. Insets show isotopic distributions aligned with experimental peaks for $(DNA)_2[Ag_{15}]^{9+}$ at z = 5− (light blue) and z = 4− (deep blue). Isotopic distributions were calculated using the chemical formula $C_{192}H_{244}N_{78}O_{110}P_{18}Ag_{15}$. Reproduced from Ref. 1.[1]

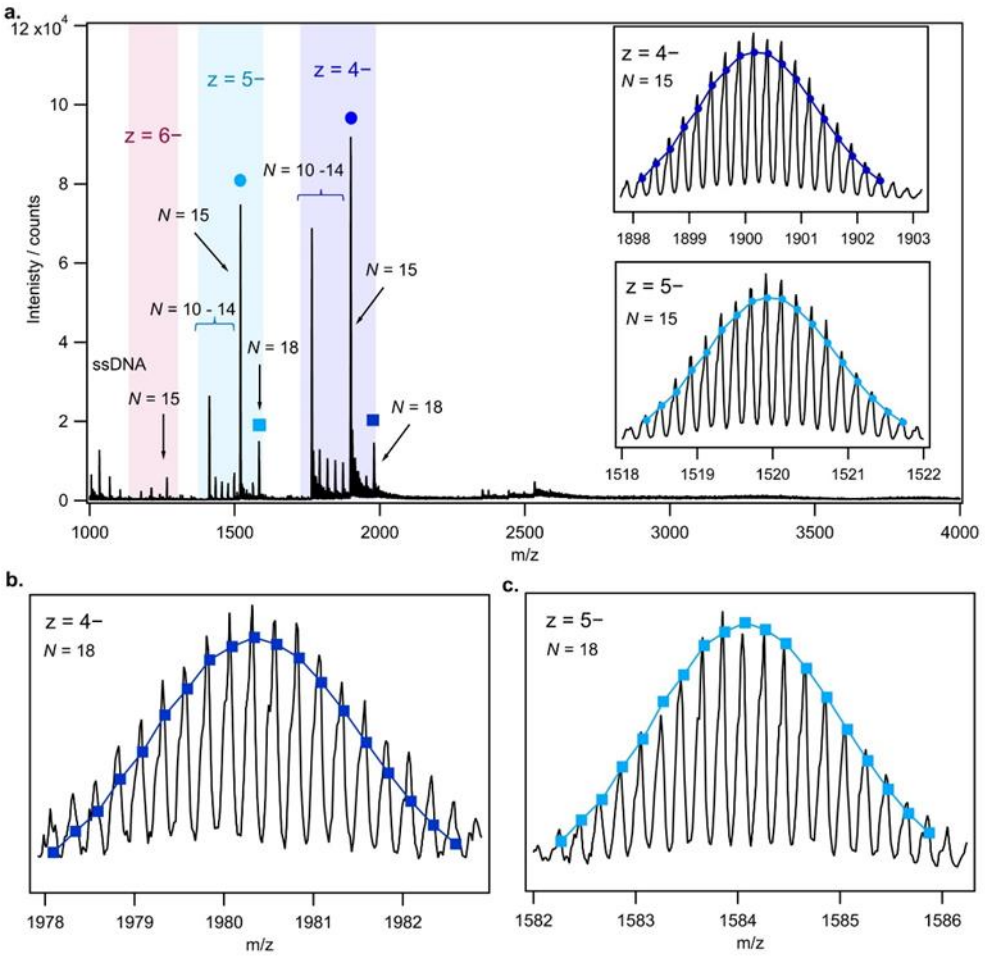

Figure S5. Mass spectra of ***I*.3**.[4] **a.** Experimental isotopic distributions (black curves) for all peaks of ***I*.3** mass spectra. Insets show isotopic distributions aligned with experimental peaks for $(DNA)_2[Ag_{15}]^{9+}$ at z = 5− (light blue, circled) and z = 4− (deep blue, circled) for the peaks with the highest intensity. **b**) and **c**) Isotopic distributions with experimental peaks for $(DNA)_2[Ag_{18}]^{12+}$ at z = 4− (deep blue, squares) and z = 5− (light blue, squares), respectively. Isotopic distributions were calculated using the chemical formula $C_{190}H_{242}N_{80}O_{112}P_{18}Ag_{15}$ (**a**. insets) and $C_{190}H_{242}N_{80}O_{112}P_{18}Ag_{18}$ (for **b.** and **c.**), respectively. Reproduced from Ref. 1.[1]

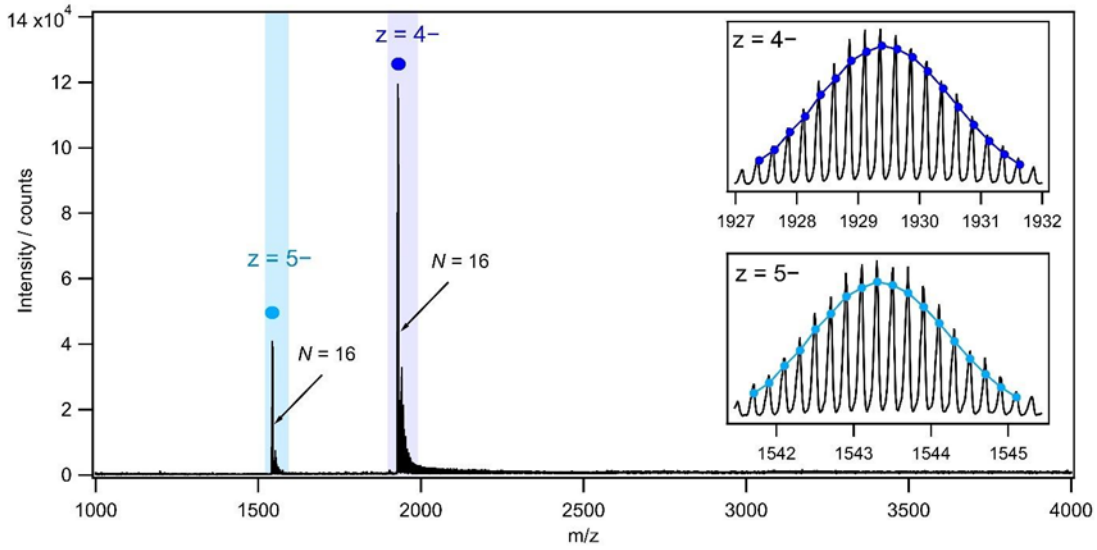

Figure S6. Mass spectra of ***I*.4.** Experimental isotopic distributions (black curves) for all peaks of ***I*.4** mass spectra. Insets show isotopic distributions aligned with experimental peaks for $(DNA)_2[Ag_{16}]^{10+}$ at z = 5− (light blue) and z = 4− (deep blue). Isotopic distributions were calculated using the chemical formula $C_{194}H_{248}N_{80}O_{118}P_{18}Ag_{16}$. Reproduced from Ref. 1.[1]

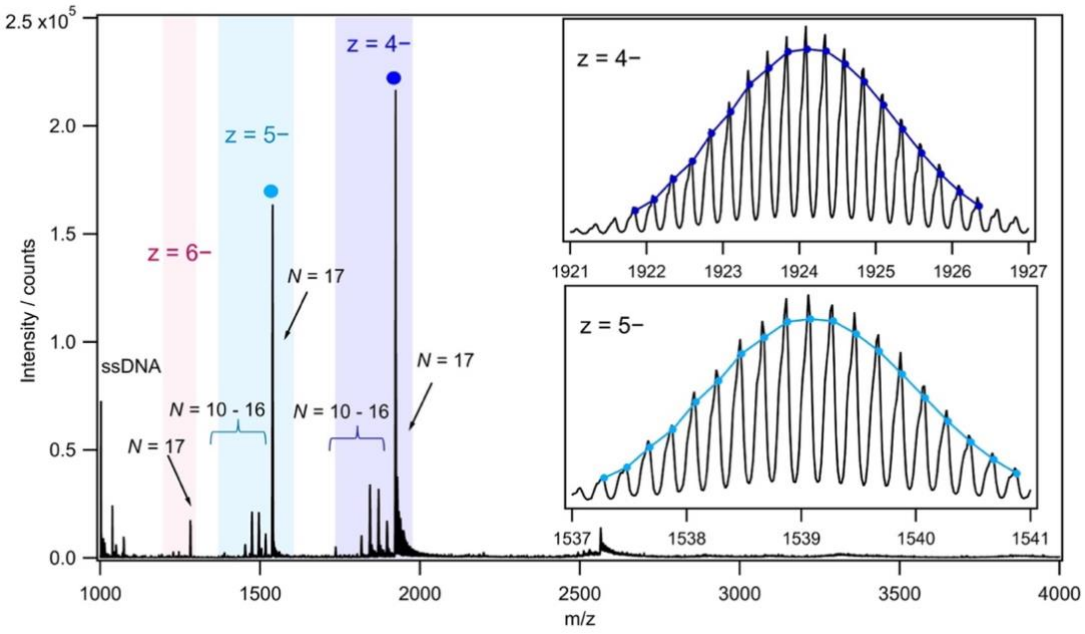

Figure S7. Mass spectra of ***I*.5.** Experimental isotopic distributions (black curves) for all peaks of ***I*.5** mass spectra. Insets show isotopic distributions aligned with experimental peaks for $(DNA)_2[Ag_{17}]^{11+}$ at z = 5− (light blue) and z = 4− (deep blue). Isotopic distributions were calculated using the chemical formula $C_{190}H_{248}N_{62}O_{120}P_{18}Ag_{17}$. Reproduced from Ref. 1.[1]

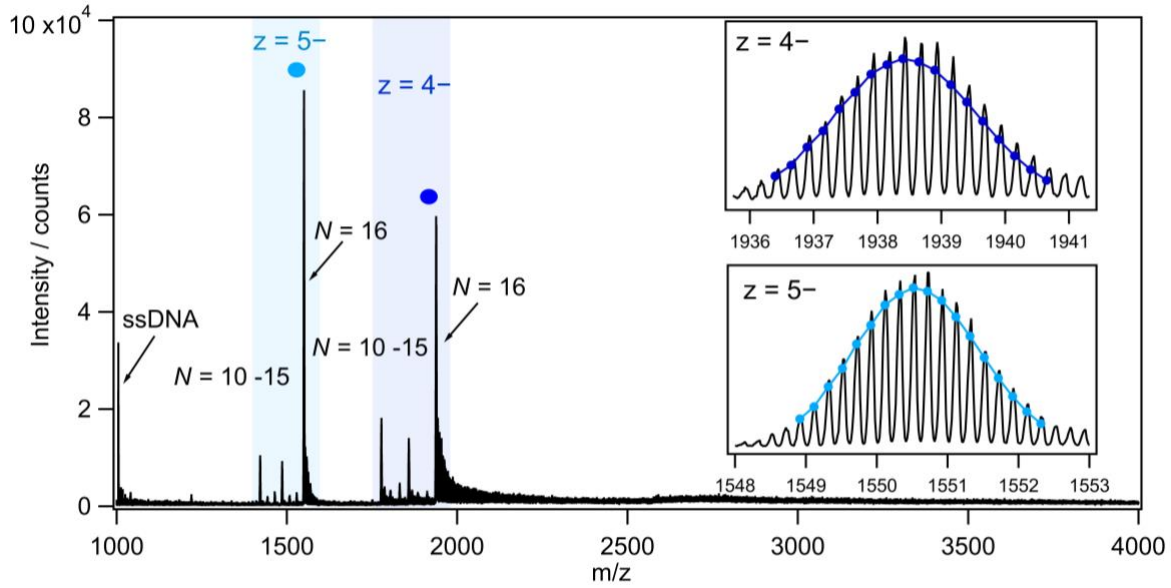

Figure S8. Mass spectra of ***I*.6.**[4] Experimental isotopic distributions (black curves) for all peaks of ***I*.5** mass spectra. Insets show isotopic distributions aligned with experimental peaks for $(DNA)_2[Ag_{16}]^{10+}$ at z = 5− (light blue) and z = 4− (deep blue). Isotopic distributions were calculated using the chemical formula $C_{194}H_{244}N_{82}O_{110}P_{18}Ag_{16}$. Reproduced from Ref. 1.[1]

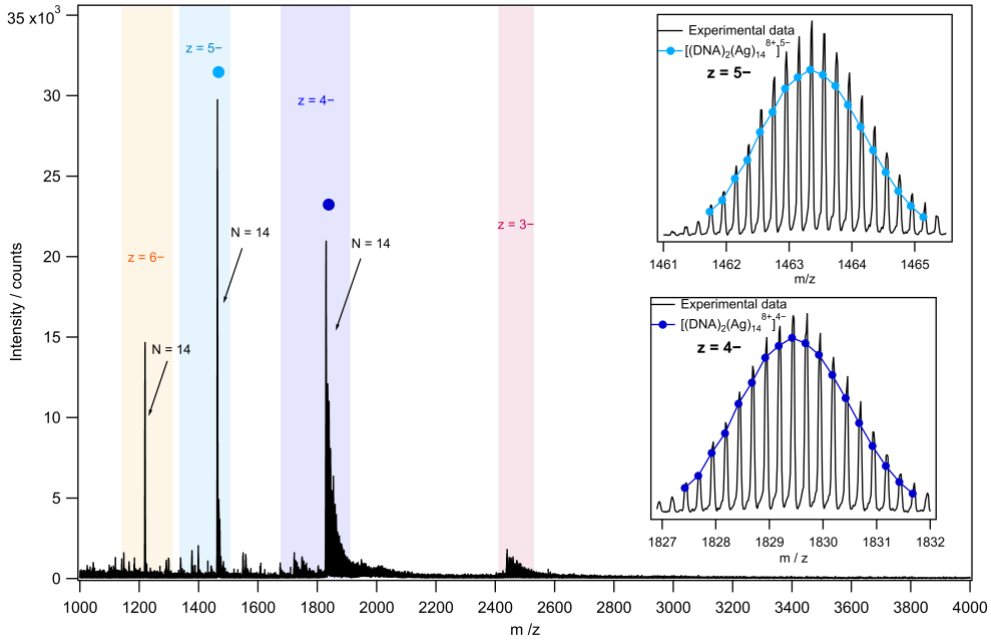

Figure S9. Mass spectra of ***I*.7.**[1] Experimental isotopic distributions (black curves) for all peaks of ***I*.5** mass spectra. Insets show isotopic distributions aligned with experimental peaks for $(DNA)_2[Ag_{14}]^{8+}$ at z = 5− (light blue) and z = 4− (deep blue). Isotopic distributions were calculated using the chemical formula $C_{184}H_{242}N_{68}O_{116}P_{18}Ag_{14}$. Reproduced from Ref. 2.[2]

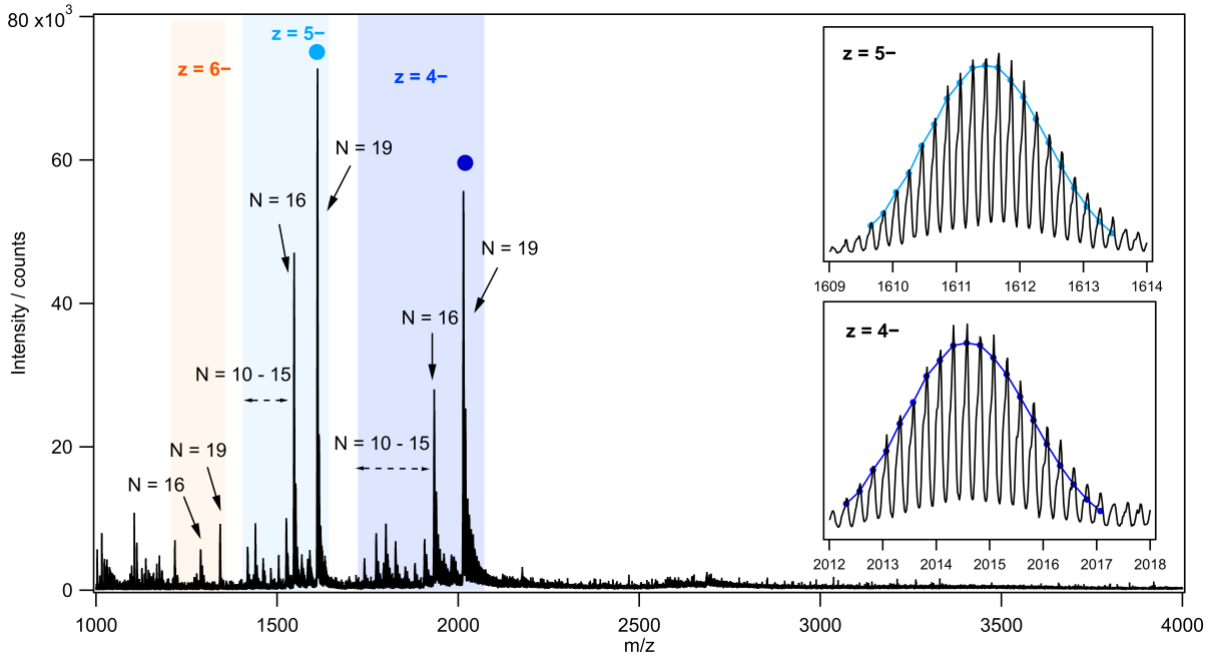

Figure S10. Mass spectra of ***I*.8** Experimental isotopic distributions (black curves) for all peaks of ***I*.5** mass spectra. Insets show isotopic distributions aligned with experimental peaks for $(DNA)_2[Ag_{19}]^{13+}$ at z = 5− (light blue) and z = 4− (deep blue). Isotopic distributions were calculated using the chemical formula $C_{192}H_{244}N_{78}O_{114}P_{18}Ag_{19}$.

3.2.2 Mass spectra of Group II Ag_N-DNAs.

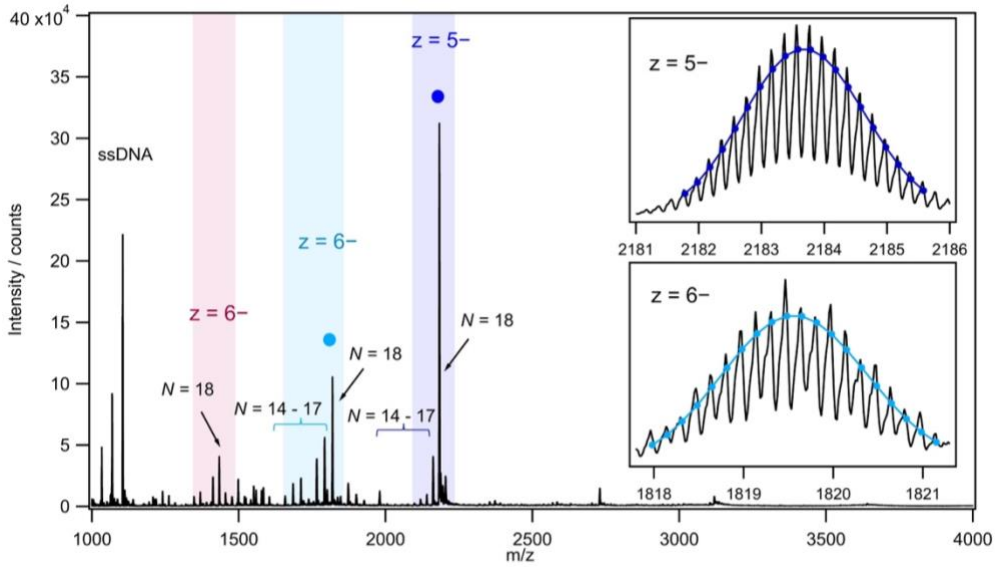

Figure S11. Mass spectra of ***II*.1.** Experimental isotopic distributions (black) for all peaks of ***II*.1** mass spectra. Insets show isotopic distributions aligned with experimental peaks for $(DNA)_3[Ag_{18}]^{12+}$ at z = 6− (light blue) and z = 5− (deep blue). Isotopic distributions were calculated using the chemical formula $C_{285}H_{363}N_{120}O_{168}P_{27}Ag_{18}$. Reproduced from Ref. 1.[1]

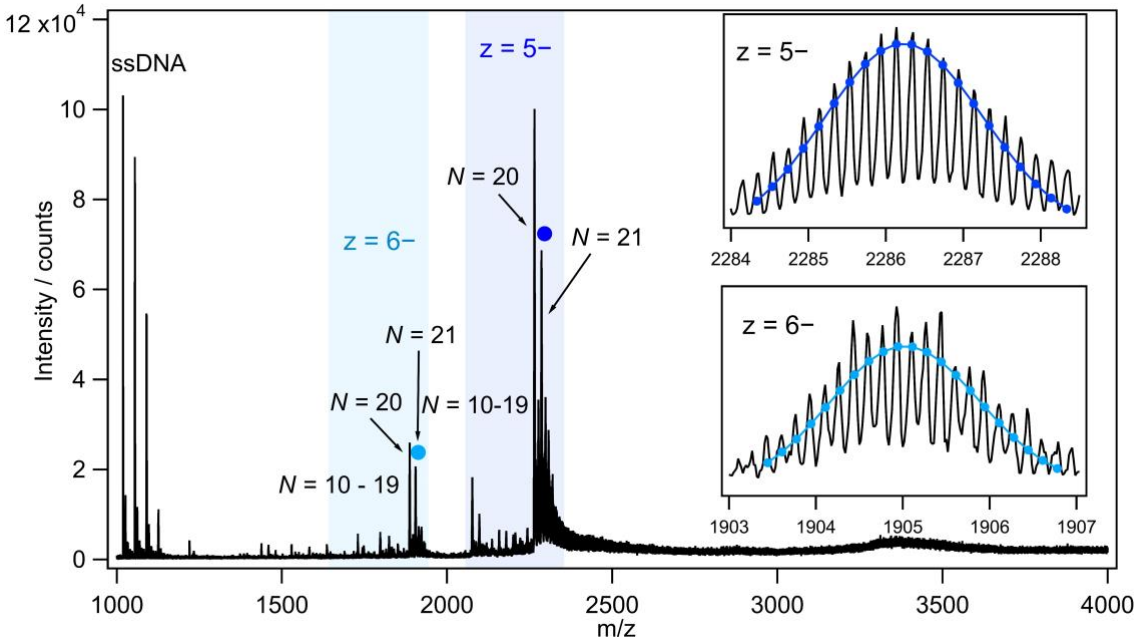

Figure S12. Mass spectra of ***II*.2**. Experimental isotopic distributions (black curves) for all peaks of ***II*.3** mass spectra. Insets show isotopic distributions aligned with experimental peaks for $(DNA)_3[Ag_{21}]^{15+}$ at z = 6− (light blue) and z = 5− (deep blue). Isotopic distributions were calculated using the chemical formula $C_{291}H_{363}N_{132}O_{165}P_{27}Ag_{21}$. Reproduced from Ref. 1.[1]

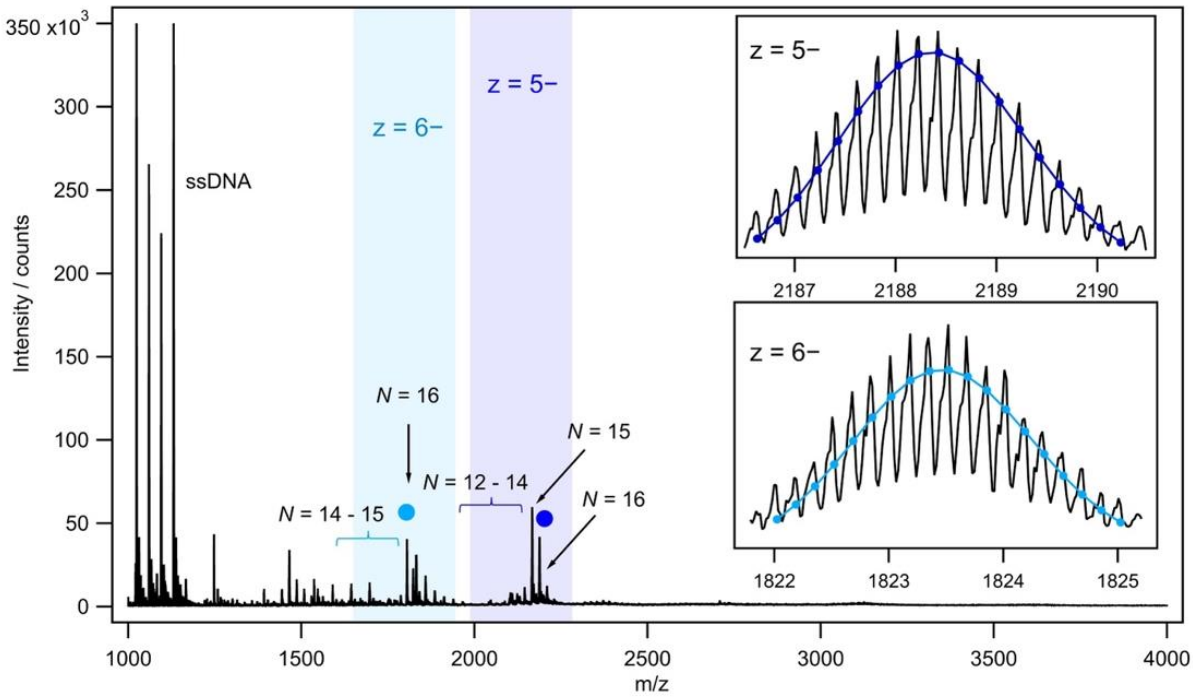

Figure S13. Mass spectra of ***II*.3**. Experimental isotopic distributions (black curves) for all peaks of ***II*.3** mass spectra. Insets show isotopic distributions aligned with experimental peaks for $(DNA)_3[Ag_{16}]^{10+}$ at z = 6− (light blue) and z = 5− (deep blue). Isotopic distributions were calculated using the chemical formula $C_{294}H_{366}N_{129}O_{168}P_{27}Ag_{16}$. Reproduced from Ref. 1.[1]

3.2.3 Mass spectra of Group III Ag_N-DNAs.

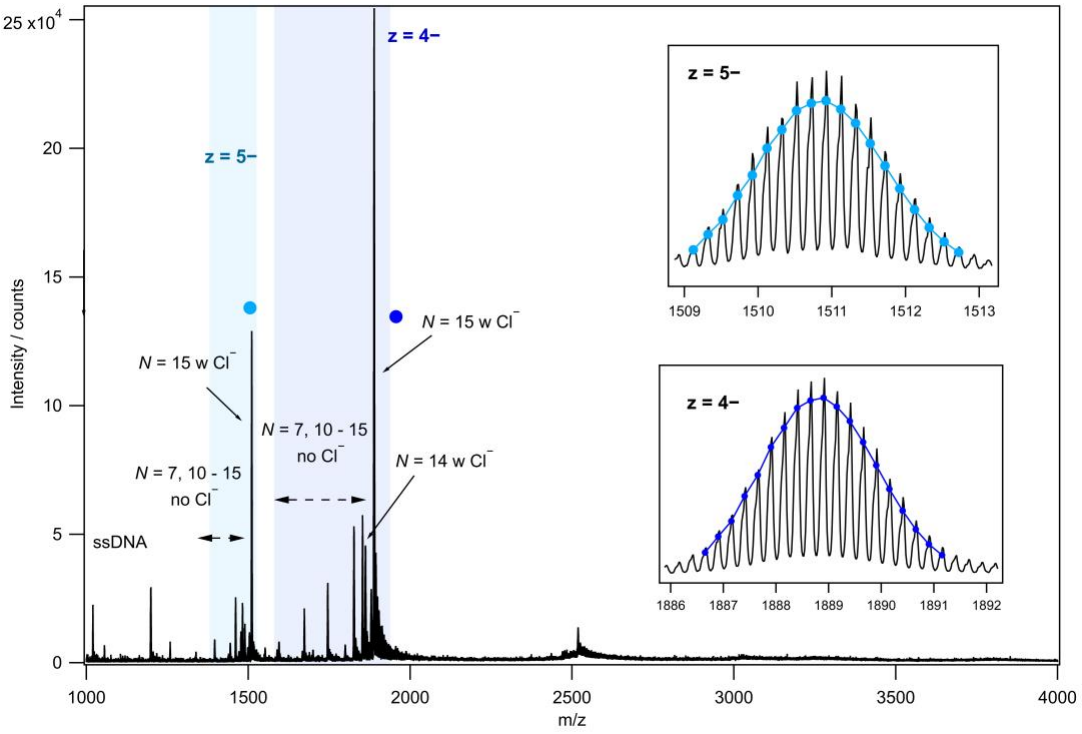

Figure S14. Mass spectra of ***III*.1**. Experimental isotopic distributions (black curves) for all peaks of ***III*.3** mass spectra. Insets show isotopic distributions aligned with experimental peaks for $(DNA)_2[Ag_{15}]^{91+}$ at z = 6− (light blue) and z = 5− (deep blue). Isotopic distributions were calculated using the chemical formula $C_{294}H_{366}N_{129}O_{168}P_{27}Ag_{15}Cl$. Reproduced from Ref. 4.[4]

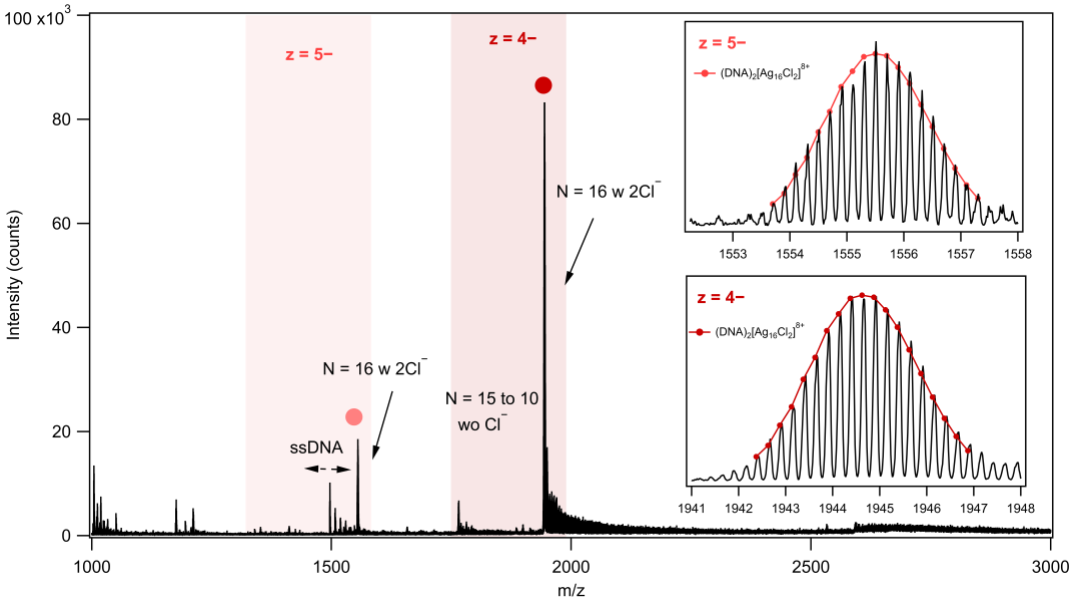

Figure S15. Mass spectra of ***III*.2**. [3] Experimental isotopic distributions (black curves) for all peaks of ***III*.3** mass spectra. Insets show isotopic distributions aligned with experimental peaks for $(DNA)_2[Ag_{16}]^{10+}$ at z = 6− (light red) and z = 5− (dark red). Isotopic distributions were calculated using the chemical formula $C_{294}H_{366}N_{129}O_{168}P_{27}Ag_{16}Cl_2$. Reproduced from Ref. 4.[4]

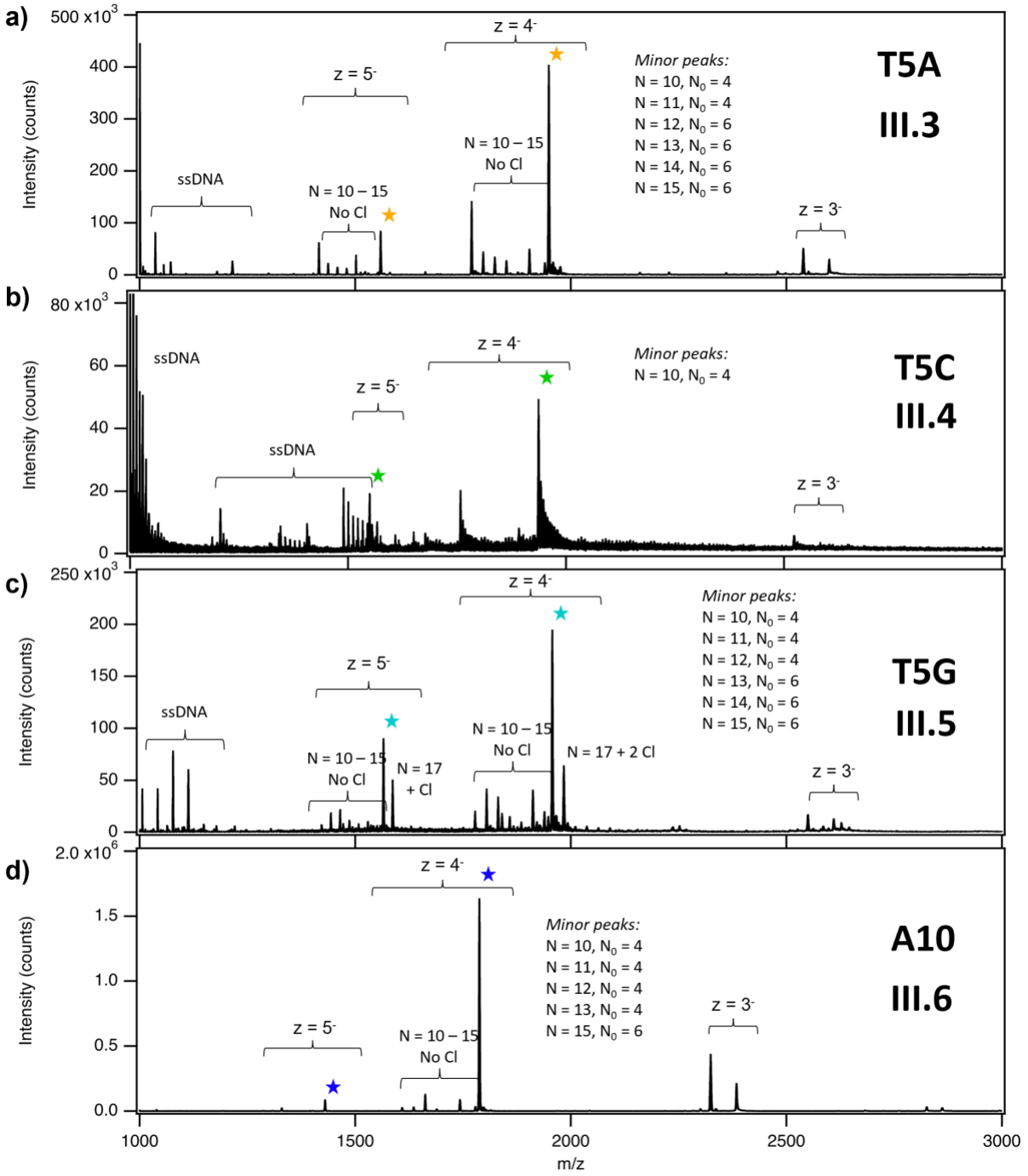

Figure S16. Mass spectra of ***III*.3** to ***III*.6**. Reproduced from Ref. 4.[4]

3.2.4 Mass spectra of Group IV Ag_N-DNAs.

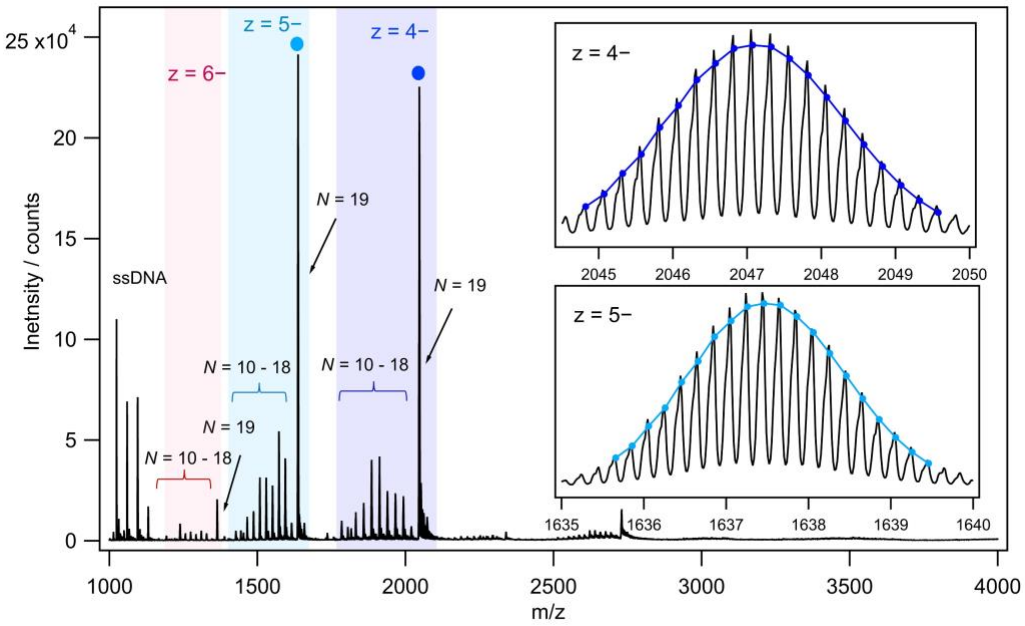

Figure S17. Mass spectra of ***IV*.1.**[4] Experimental isotopic distributions (black curves) for peaks of ***IV*.1** mass spectra. Insets show isotopic distributions aligned with experimental peaks for $(DNA)_2[Ag_{19}]^{11+}$ at z = 5− (light blue) and z = 4− (deep blue), as indicated by circles. Isotopic distributions were calculated using the chemical formula $C_{196}H_{244}N_{86}O_{112}P_{18}Ag_{19}$. Reproduced from Ref. 1.[1]

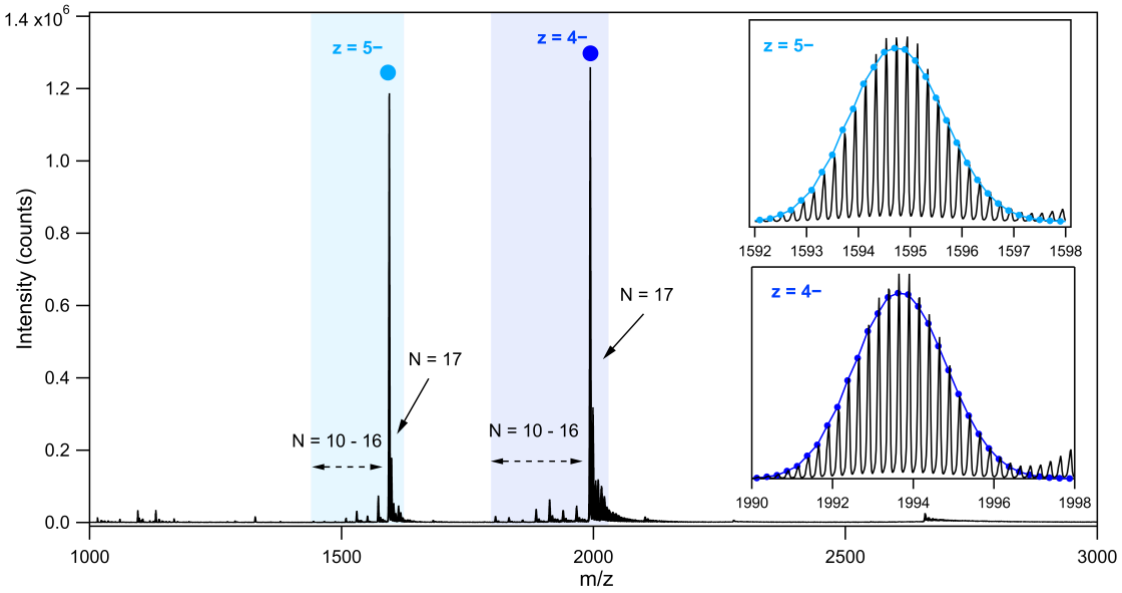

Figure S18. Mass spectra of ***IV*.2.**[2] Experimental isotopic distributions (black curves) for peaks of ***IV*.2** mass spectra. Insets show isotopic distributions aligned with experimental peaks for $(DNA)_2[Ag_{17}]^{9+}$ at z = 5− (light blue) and z = 4− (deep blue), as indicated by circles. Isotopic distributions were calculated using the chemical formula $C_{196}H_{244}N_{86}O_{112}P_{18}Ag_{17}$. Reproduced from Ref. 3.[3]

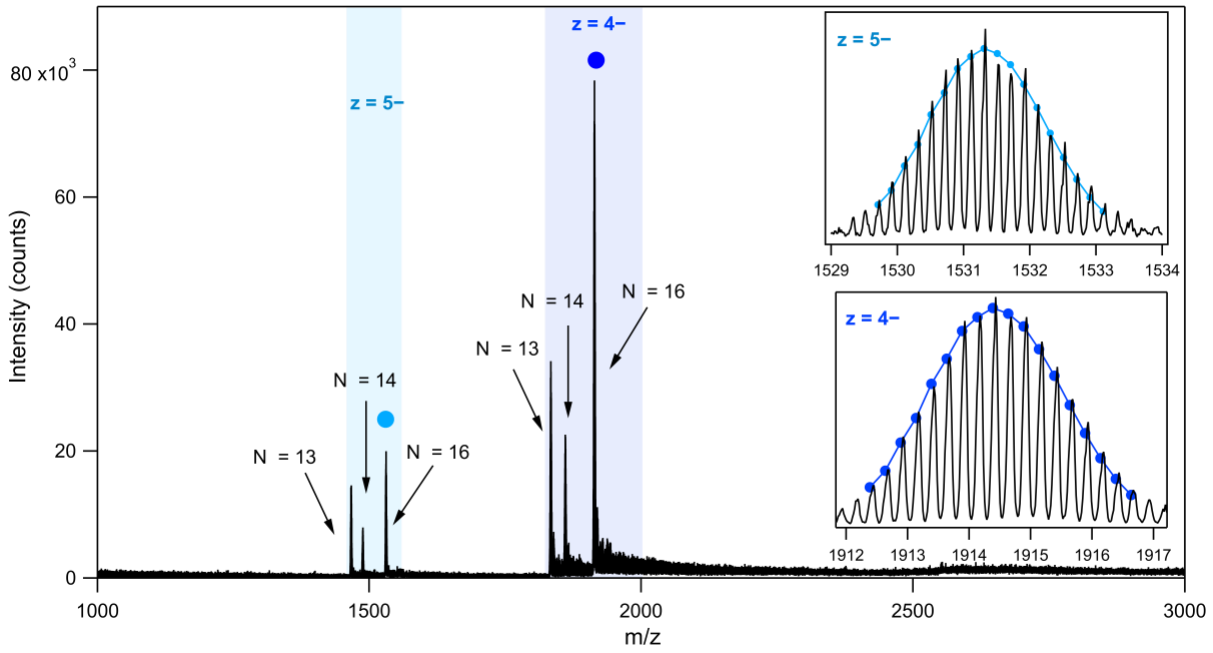

Figure S19. Mass spectra of ***IV*.3.**[2] Experimental isotopic distributions (black curves) for peaks of ***IV*.3** mass spectra. Insets show isotopic distributions aligned with experimental peaks for $(DNA)_2[Ag_{16}]^{8+}$ at z = 5− (light blue) and z = 4− (deep blue), as indicated by circles. Isotopic distributions were calculated using the chemical formula $C_{129}H_{246}N_{72}O_{114}P_{18}Ag_{16}$. Reproduced from Ref. 3.[3]

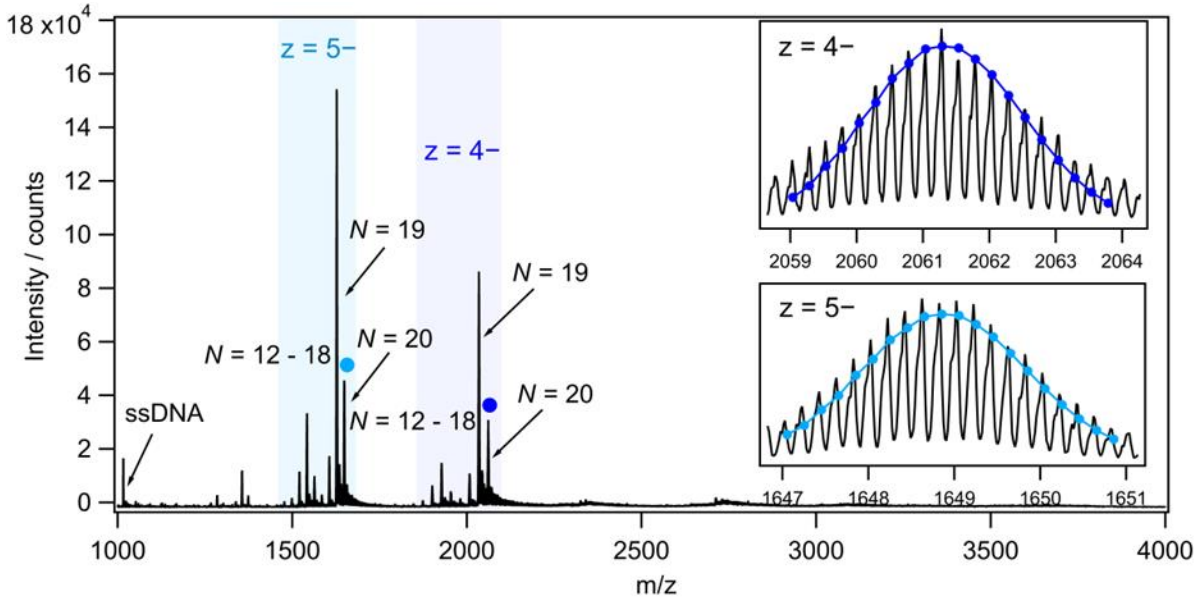

Figure S20. Mass spectra of ***IV*.4.**[4] Experimental isotopic distributions (black curves) for peaks of ***IV*.4** mass spectra. Insets show isotopic distributions aligned with experimental peaks for $(DNA)_2[Ag_{20}]^{12+}$ at z = 5− (light blue) and z = 4− (deep blue), as indicated by circles. Isotopic distributions were calculated using the chemical formula $C_{196}H_{246}N_{80}O_{114}P_{18}Ag_{20}$. Reproduced from Ref. 1.[1]

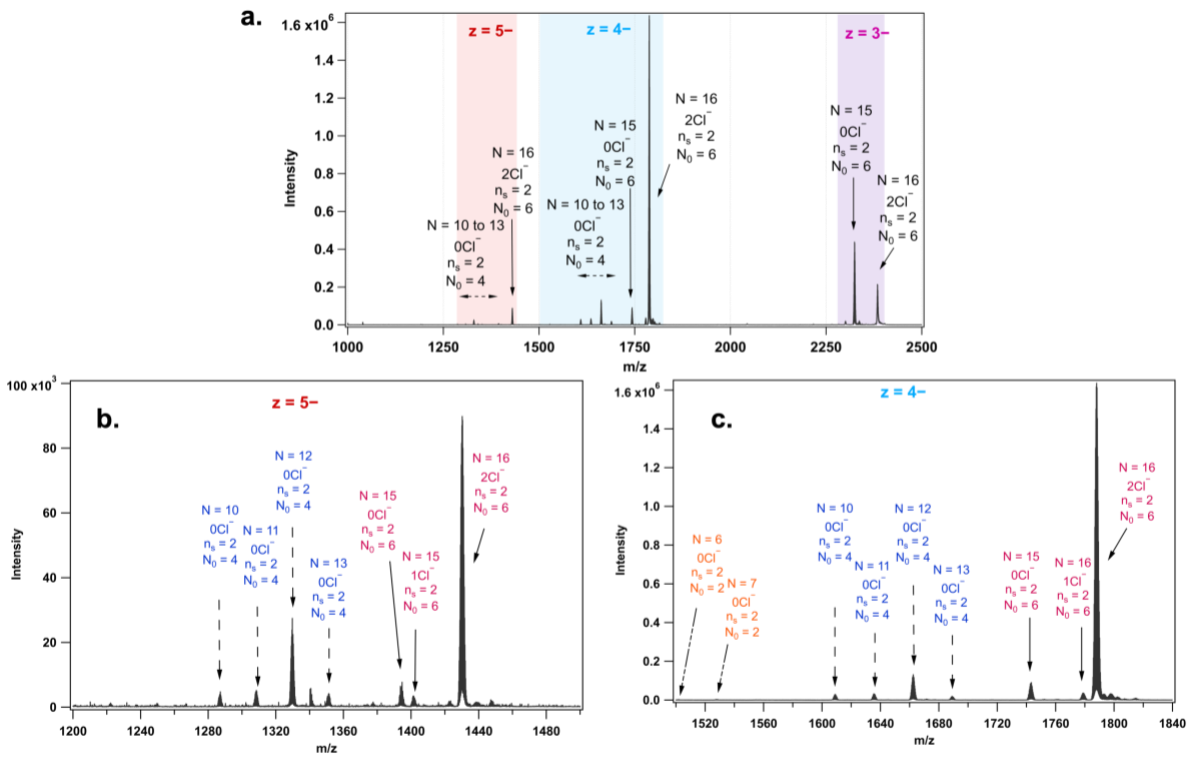

Figure S21. a) Mass spectra of **III.6**: charge states (z) = 3−, 4−, and 5− are shaded with colors, purple, blue, and red, respectively. **b)** and **c)** zoomed-in mass spectra of **III.6** for charge states, z = 5− and 4−, respectively. The molecular composition of each peak with their corresponding n_s, N, and N_0 values are indicated.

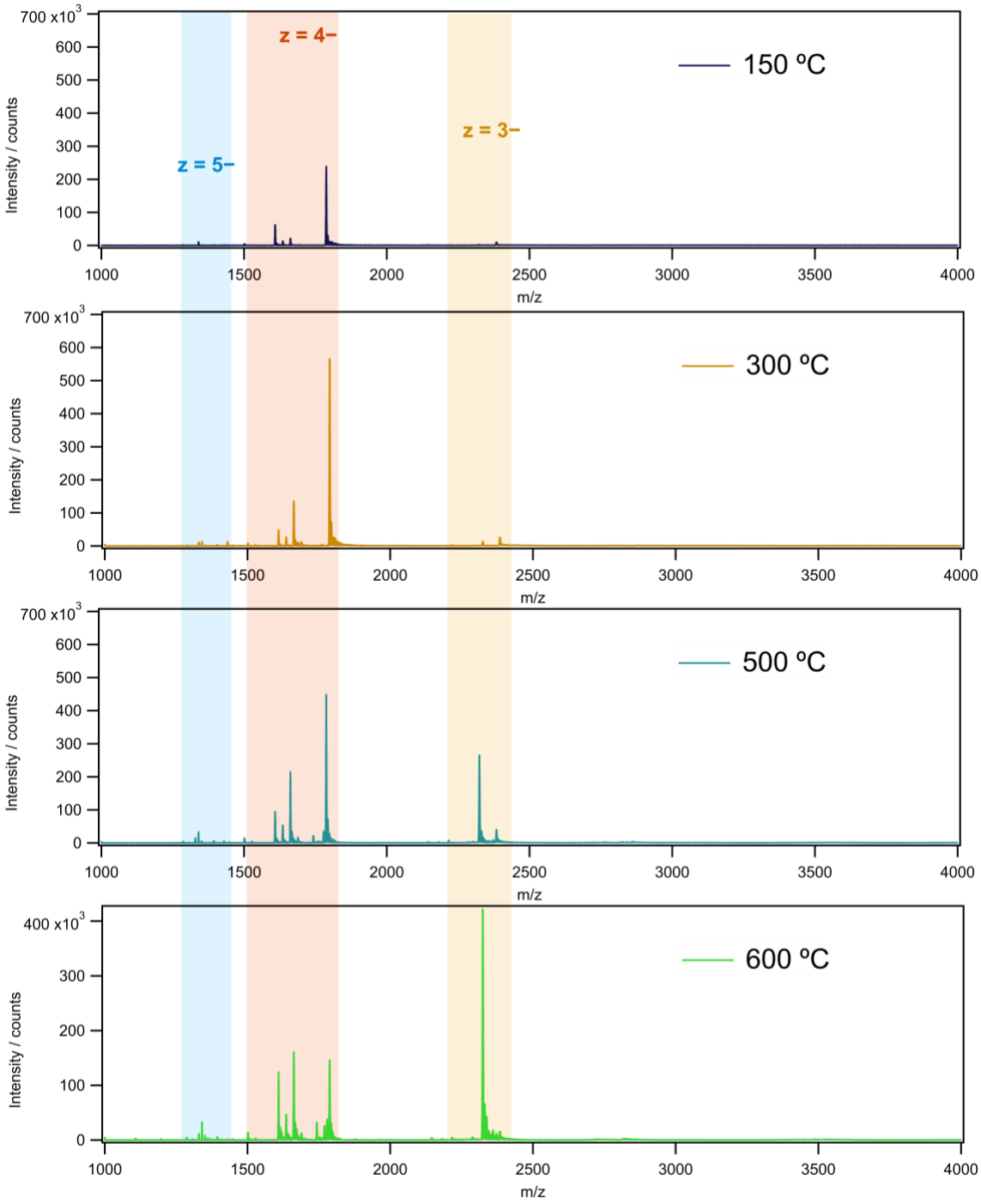

Figure S22. Mass spectra of **III.6**, were obtained at a source temperature of 80 ºC and desolvation temperatures ranging from 150 ºC to 600 ºC. The intensity of peaks with z = 3− increases with the increase in desolvation energy.

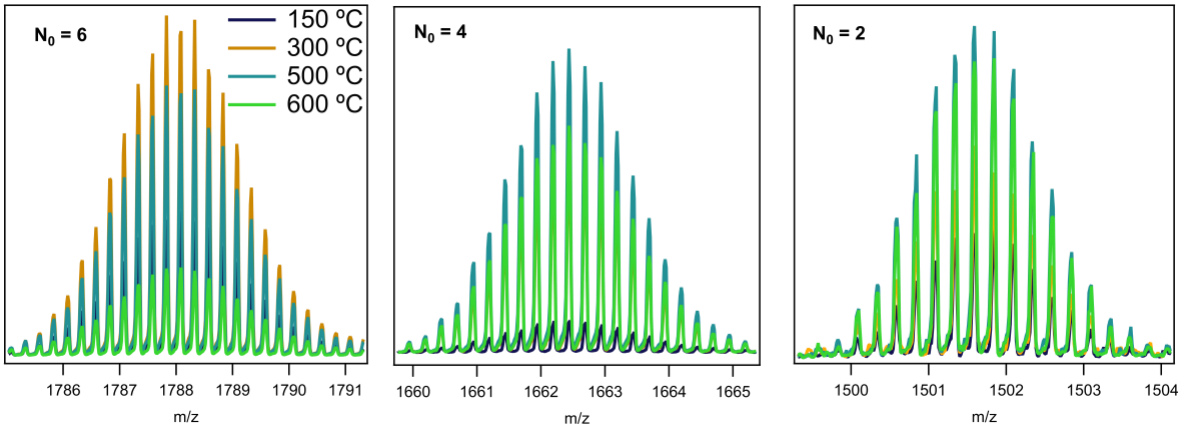

Figure S23. Comparison of N_0 values of peaks at z = 4– for **III.6** mass spectra obtained at different desolvation temperatures (full mass spectra shown in **Fig. S22**) at 80 ºC source temperature.

Table S1. Summary of center of Gaussian fits of the peaks in the experimentally measured mass spectra of **III.6** (**Fig. S23**) for different desolvation temperatures.

N_0	Desolvation temperature (°C)	Gaussian fits
N_0 = 6	150	1788.1 ± 0.107
	300	1788.1 ± 0.112
	500	1788.1 ± 0.111
	600	1788.1 ± 0.112
N_0 = 4	150	1662.5 ± 0.119
	300	1662.4 ± 0.122
	500	1662.4 ± 0.122
	600	1662.4 ± 0.123
N_0 = 2	150	1501.7 ± 0.101
	300	1501.6 ± 0.101
	500	1501.6 ± 0.101
	600	1501.6 ± 0.0995

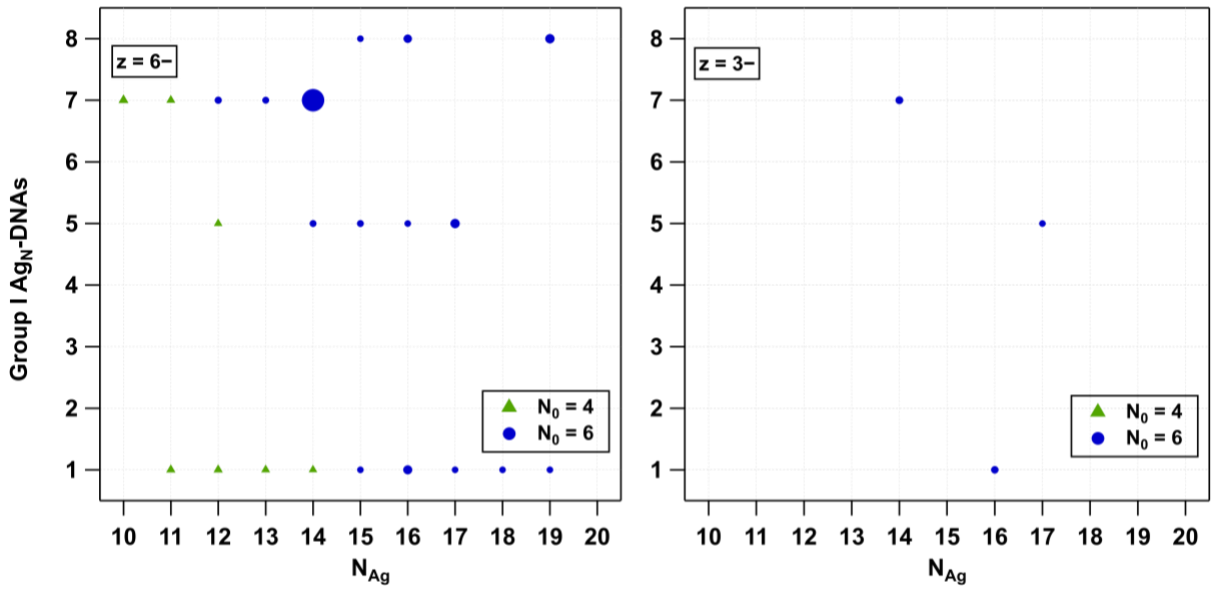

Figure S24. N_0 vs. N_{Ag} plot for **Group I** Ag$_N$-DNAs at z = 6– and z = 3–. The type of markers shows the N_0 values (blue circles and green triangles for N_0 = 6 and 4, respectively) and the size of the marker denotes the intensity of the peaks in the mass spectra. Note: All the peaks indicated with different N_{Ag} are stabilized by two ssDNA, *i.e.*, n_s = 2.

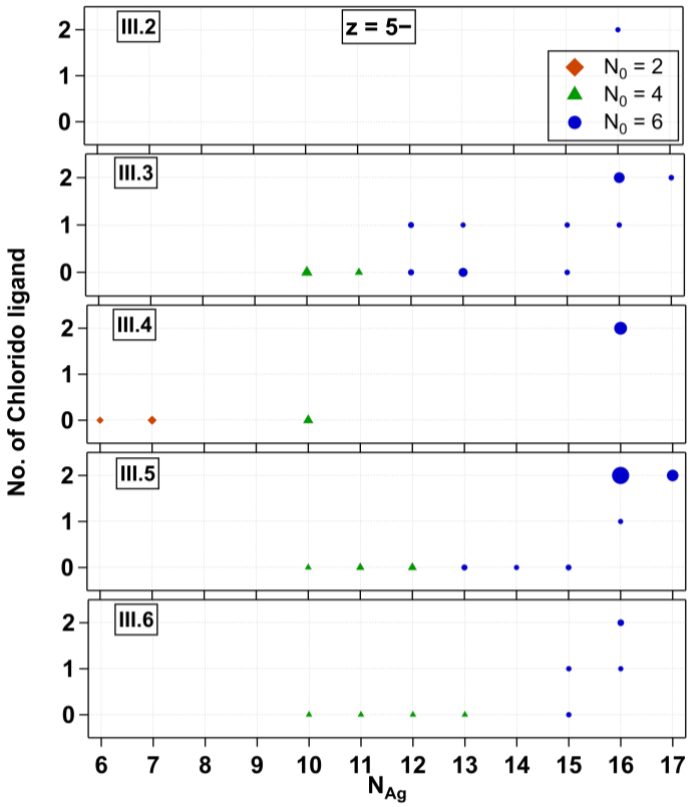

Figure S25. The plot of N_0 values *vs*. N_{Ag} for peaks with different numbers of chlorido ligands for **Group III** Ag$_N$-DNAs at z = 5–. The type of markers shows the N_0 values (blue circles, green triangles, and ochre diamonds for N_0 = 6, 4, and 2, respectively) and the size of the marker

denotes the intensity of the peaks in the mass spectra. Note: all the peaks indicated with different N_{Ag} are stabilized by two ssDNA, *i.e.*, n_s = 2.

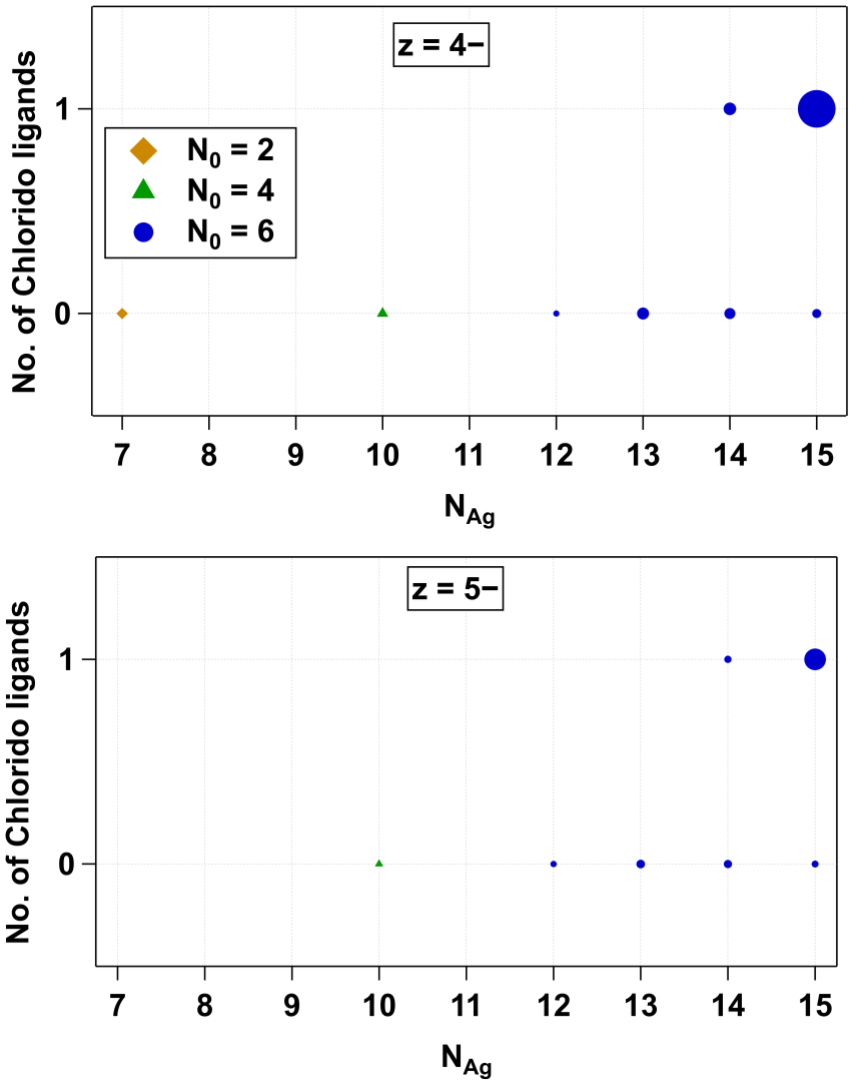

Figure S26. The plot of N_0 values *vs*. N_{Ag} for peaks with different numbers of chlorido ligands for **III.1**.The type of markers shows the N_0 values (blue circles, green triangles, and ochre diamonds for N_0 = 6, 4, and 2, respectively) and the size of the marker denotes the intensity of the peaks in the mass spectra. Note: All the peaks indicated with different N_{Ag} are stabilized by two ssDNA, *i.e.*, n_s = 2.

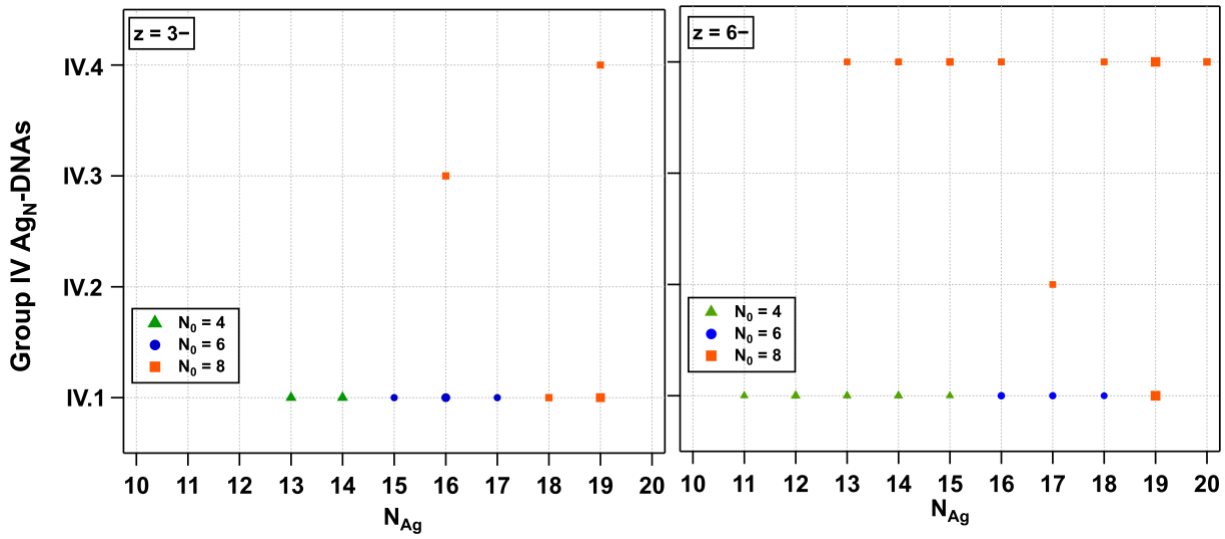

Figure S27. The plot of N_0 values *vs*. N_{Ag} for **Group IV** Ag_N-DNAs at z = 6– and 3–The type of markers shows the N_0 values (orange squares, blue circles, and green triangles for N_0 = 8, 6, and 4, respectively) and the size of the marker denotes the intensity of the peaks in the mass spectra. Note: All the peaks indicated with different N_{Ag} are stabilized by two ssDNA, *i.e.*, n_s = 2.

4 Computational modeling

Calculations were done using density functional theory (DFT) as implemented in software GPAW.[5, 6] In calculations we used real space grids with a grid spacing of 0.2 and Perdew-Burke-Ernzerhof (PBE) functional.[7] The cluster structure was created based on the experimentally solved crystal structure by Vosch, *et. al*.[8] which later was confirmed to include 2 Cl^- ligands on the Ag core surface and computationally analyzed as a corrected model structure.[9, 10] Hence, the same model structure is considered here also. In all calculations we used implicit water solvent model at the background.[11, 12] PBE optimized coordinates of the cluster (optimization criterion: forces of atoms below 0.05 eV.) were used as a starting structure for the molecular dynamics simulation. Molecular dynamics (MD) was performed using Langevin thermostat with 2 fs time step and 0.01 fs friction parameter. Masses of hydrogen atoms were treated as deuterium atoms in the calculation for stability reasons and to optimize the production of the simulation length. The total length of the MD run was 14.3 ps from which heating to the target temperature of 300K took ~3 ps. To

reveal the possible fragmentation, the minimum distance between Ag_6 and Ag_{10} parts of the metal core was analyzed from the MD-trajectory. The contact area of the two parts is capped with Cl ligands. The minimum distance was determined from all Ag-Ag distances between Ag_6 and Ag_{10} structural parts at each step. In addition, the behavior of the HOMO-LUMO gap was analyzed.

The last snapshot structure was taken for more detailed analysis of the electronic structure. The further analyze of the structure was made using GLLB-SC xc-functional. The density of states was projected to spherical harmonics functions centered at the center of mass of the Ag_6 and Ag_{10} metal core structure parts separately to reveal if the electronic characteristics have changed during fragmentation. The projection was done inside a spherical cutoff region with radii of 3 and 4, respectively, for Ag_6 and Ag_{10} parts.

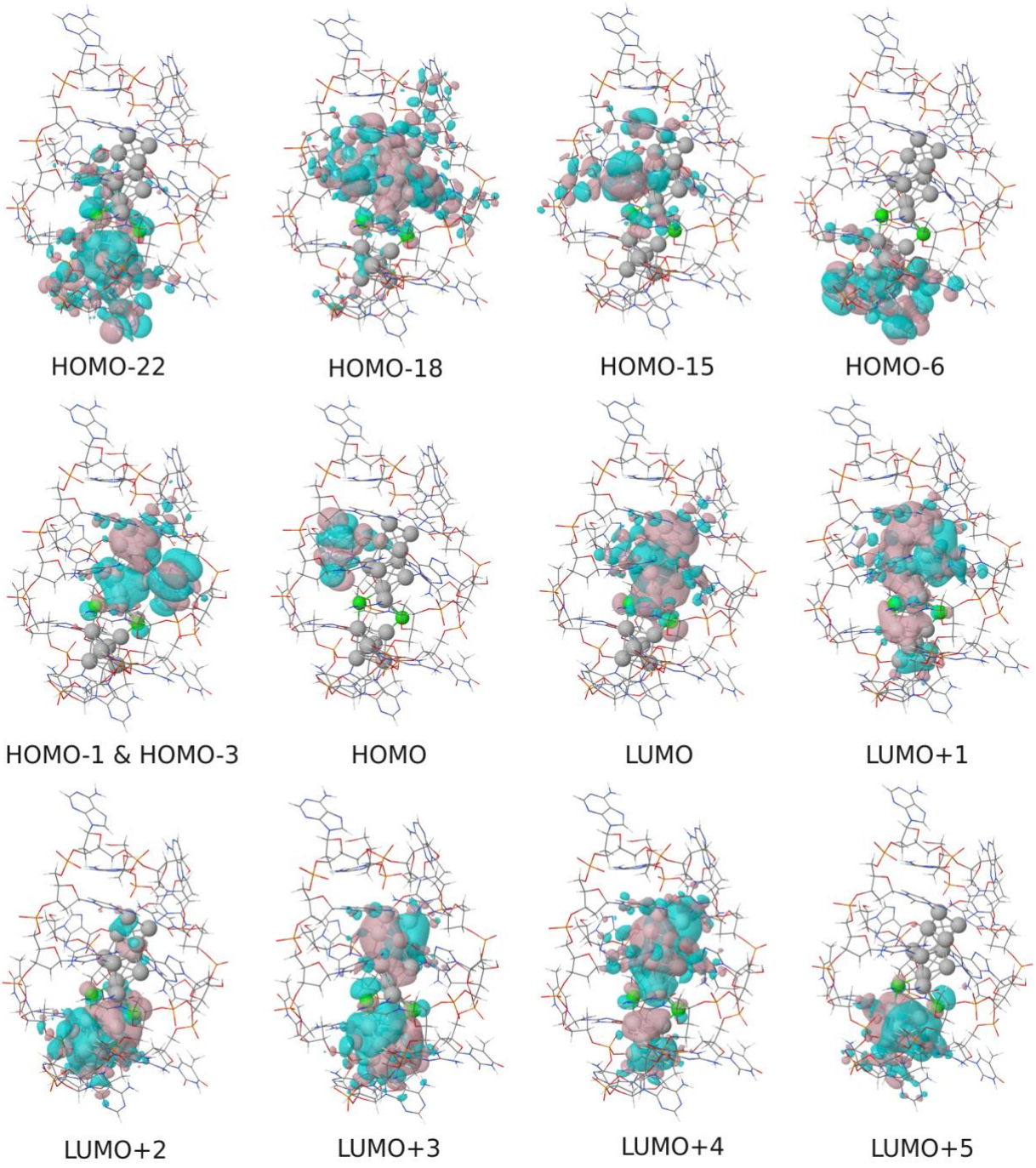

Figure S26. Frontier molecular orbitals of the III.6, $(DNA)_2(Ag_{16}Cl_2)^{8+}$ cluster calculated at GLLB-SC functional with implicit solvent.

5 References.

1. R. Guha, A. Gonzàlez-Rosell, M. Rafik, N. Arevalos, B. B. Katz and S. M. Copp, *Chem. Sci.*, 2023, **14**, 11340-11350.
2. R. Guha, M. Rafik, A. Gonzàlez-Rosell and S. M. Copp, *Chem. Commun.*, 2023, **59**, 10488-10491.
3. A. Gonzàlez-Rosell, R. Guha, C. Cerretani, V. Rück, M. B. Liisberg, B. B. Katz, T. Vosch and S. M. Copp, *J. Phys. Chem. Lett.*, 2022, **13**, 8305-8311.
4. A. Gonzàlez-Rosell, S. Malola, R. Guha, N. R. Arevalos, M. F. Matus, M. E. Goulet, E. Haapaniemi, B. B. Katz, T. Vosch, J. Kondo, H. Häkkinen and S. M. Copp, *J. Am. Chem. Soc.*, 2023, **145**, 10721-10729.
5. J. Enkovaara, C. Rostgaard, J. J. Mortensen, J. Chen, M. Dułak, L. Ferrighi, J. Gavnholt, C. Glinsvad, V. Haikola, H. A. Hansen, H. H. Kristoffersen, M. Kuisma, A. H. Larsen, L. Lehtovaara, M. Ljungberg, O. Lopez-Acevedo, P. G. Moses, J. Ojanen, T. Olsen, V. Petzold, N. A. Romero, J. Stausholm-Møller, M. Strange, G. A. Tritsaris, M. Vanin, M. Walter, B. Hammer, H. Häkkinen, G. K. Madsen, R. M. Nieminen, J. K. Nørskov, M. Puska, T. T. Rantala, J. Schiøtz, K. S. Thygesen and K. W. Jacobsen, *J. Phys. Condens. Matter*, 2010, **22**, 253202.
6. J. J. Mortensen, A. H. Larsen, M. Kuisma, A. V. Ivanov, A. Taghizadeh, A. Peterson, A. Haldar, A. O. Dohn, C. Schäfer, E. Jónsson, E. D. Hermes, F. A. Nilsson, G. Kastlunger, G. Levi, H. Jónsson, H. Häkkinen, J. Fojt, J. Kangsabanik, J. Sødequist, J. Lehtomäki, J. Heske, J. Enkovaara, K. T. Winther, M. Dulak, M. M. Melander, M. Ovesen, M. Louhivuori, M. Walter, M. Gjerding, O. Lopez-Acevedo, P. Erhart, R. Warmbier, R. Würdemann, S. Kaappa, S. Latini, T. M. Boland, T. Bligaard, T. Skovhus, T. Susi, T. Maxson, T. Rossi, X. Chen, Y. L. A. Schmerwitz, J. Schiøtz, T. Olsen, K. W. Jacobsen and K. S. Thygesen, *J. Chem. Phys.*, 2024, **160**.
7. J. P. Perdew, K. Burke and M. Ernzerhof, *Phys. Rev. Lett.*, 1996, **77**, 3865-3868.
8. C. Cerretani, J. Kondo and T. Vosch, *RSC Adv.*, 2020, **10**, 23854-23860.
9. S. Malola, M. F. Matus and H. Häkkinen, *J. Phys. Chem. C*, 2023, **127**, 16553-16559.
10. A. Held and M. Walter, *J. Chem. Phys.*, 2014, **141**, 174108.
11. M. Kuisma, J. Ojanen, J. Enkovaara and T. T. Rantala, *Phys. Rev. B*, 2010, **82**, 115106.
12. M. Walter, J. Akola, O. Lopez-Acevedo, P. D. Jadzinsky, G. Calero, C. J. Ackerson, R. L. Whetten, H. Grönbeck and H. Häkkinen, *Proc. Natl. Acad. Sci. U.S.A.*, 2008, **105**, 9157-9162.